Computational Study of Hexanal Peroxy Radical–Water Complexes

DATASET *in* INTERNATIONAL JOURNAL OF QUANTUM CHEMISTRY · APRIL 2012

Impact Factor: 1.43 · DOI: 10.1002/qua.23220

11 AUTHORS, INCLUDING:

Ryan Dabell

Brigham Young University - Idaho

12 PUBLICATIONS **128** CITATIONS

SEE PROFILE

Jaron C Hansen

Brigham Young University - Provo Main Cam…

38 PUBLICATIONS **355** CITATIONS

SEE PROFILE

Computational Study of Hexanal Peroxy Radical–Water Complexes

EMILY BURRELL,[1] JARED C. CLARK,[2] MATHEW SNOW,[1] HEIDI DUMAIS,[1] SEONG-CHEOL LEE,[1] BRAD J. NIELSON,[1] DEREK OSBORNE,[1] LUCIA SALAMANCA-CARDONA,[1] LOGAN ZEMP,[1] RYAN S. DABELL,[1] JARON C. HANSEN[2]

[1]*Department of Chemistry, Brigham Young University-Idaho, Rexburg, ID 83460*

[2]*Department of Chemistry and Biochemistry, Brigham Young University, Provo, UT 84602*

Received 16 March 2011; accepted 16 June 2011
Published online 29 August 2011 in Wiley Online Library (wileyonlinelibrary.com).
DOI 10.1002/qua.23220

ABSTRACT: The results of an ab initio study on a family of hydroxy peroxy radical–water complexes formed from the oxidation of E-2-hexenal, which constitutes an important component of biogenic atmospheric emissions, are reported. Binding energies for the β-hydroxy-γ-peroxy hexanal (β- and γ-positions are relative to the carbonyl) radical–water complex and the γ-hydroxy-β-peroxy hexanal radical–water complex are predicted to be to 3.8 and 3.6 kcal/mol, respectively, computed at the MP2/6-311++G(2d,2p)//B3LYP/6-311++G(2d,2p) computational level. Natural bond orbital reveals that conventional hydrogen bonding between the water and the hydroxy and aldehyde functional groups of the radical are primarily responsible for the stability of the complex. It can be shown that the peroxy moiety contributes very little to the stability of the radical–water complexes. Thermochemistry calculations reveal estimated equilibrium constants that are comparable to those recently reported for several hydroxy isoprene radical–water complexes. The results of this report suggest that the hexanal peroxy radical–water complexes are expected to play a significant role in the complex chemistry of the atmosphere. Int J Quantum Chem 112: 1936–1944, 2012

Key words: peroxy hexanal radical; radical–molecule complex; 2-E-hexenal

Correspondence to: J. C. Hansen; e-mail: jhansen@chem.byu.edu

Contract grant sponsor: National Science Foundation.
Contract grant number: 0924146.

Additional Supporting Information may be found in the online version of this article.

Introduction

Organic peroxy radicals are formed from the oxidation of hydrocarbons under atmospheric conditions, and they represent an important class of intermediates leading to the formation of tropospheric ozone and nitrogen oxides (NO_x), demonstrated below:

$$RO_2 + NO \rightarrow RO + NO_2 \quad (1)$$

$$NO_2 + h\nu \rightarrow NO + O \quad (2)$$

$$O + O_2 \rightarrow O_3 \quad (3)$$

A number of studies have both theoretically predicted the presence of peroxy radical–water complexes and confirmed their existence in the laboratory. The simplest of these, the HO_2–H_2O complex, was first detected in a supersonic jet using Fourier transform microwave spectroscopy [1]. Using high-level ab initio calculations, Aloisio and Francisco reported the binding energy (−6.9 kcal/mol for the complex) for the HO_2–H_2O complex with the associated minimum energy structure [2]. Kinetic studies using laser flash photolysis coupled with UV time-resolved absorption spectroscopy have demonstrated that the HO_2 self-reaction rate increases in the presence of water vapor [3]. It is speculated that the measured increase in the reaction rate coefficient is due to the formation of the HO_2–H_2O complex as one step in the reaction mechanism. A similar rate enhancement is also observed for the HO_2 self-reaction in the presence of CH_3OH and NH_3, but not CH_4 [4–6], suggesting that such enhancements are likely the result of O—H···O or N—H···O hydrogen-bond interactions between the radical and the interacting species.

The role of the HO_2–H_2O complex has also been found to play an important part in the chemistry of other atmospheric systems. The HO_2–H_2O complex is thought to play a role in the reaction of HO_2 with NO. Turbulent flow reactor experiments have been reported that demonstrate an enhancement of the HNO_3 production channel of the $NO + HO_2 \rightarrow HNO_3$ reaction in the presence of water vapor [7]. The results further indicate that the obtained branching fraction of the HNO_3-forming channel increases from ∼ 0.2 to ∼ 7%. HO_2–H_2O has also been investigated in the context of the $SO_3 + HO_2$ reaction [8]. The primary product of this reaction is the formation of the HSO_5 radical. In the presence of water vapor, the product channel is reported to shift toward the formation of H_2SO_4, which accounts for ∼ 66% of the products form. Additionally, ab initio methods used by Long et al. [9] predict that the HO_2–H_2O complex serves to lower the decomposition barrier of CF_3OH in the atmosphere from 45.7 to ∼ 0 kcal/mol. The rate constant calculated from this work suggests that the decomposition of CF_3OH by HO_2–H_2O is the main sink for this molecule in the atmosphere.

Computational studies clarify the nature of these specific interactions. Recent computational results by Clark et al. suggest that many methyl- and ethyl-sized peroxy radicals exhibit binding energies between −2.5 and −5.1 kcal/mol with water vapor [10]. These strong binding energies are traced to the formation of hydrogen bonds between the radical's peroxy and hydroxy moieties and water, as well as surprisingly strong CH—O interactions between the radical and water that contribute up to 36% of the overall stabilization energy [10].

Using the previous studies as a foundation, theoretical investigations have focused on larger organic molecules that play essential roles in atmospheric chemistry. In recent work, Clark et al. reported the binding energies and minimum energy structures for six different hydroxy isoprene peroxy (HIP) radicals that form complexes with water, with binding energies ranging from 3.9 to 5.7 kcal/mol [11]. Using a combination of the binding energies and natural bond orbital (NBO) analyses, they hypothesized that water complexation could potentially perturb the kinetics and product branching ratios of reactions involving these species. Their results showed that larger molecular weight organic peroxy radicals could form complexes with water in much the same way that smaller radicals such as HO_2 can complex with water.

Although isoprene is the single greatest nonmethane biogenically emitted hydrocarbon, many other large organic peroxy radicals are present at significant quantities in the atmosphere. One of these species is E-2-hexenal (E2HEX), a natural product of trees, algae, and other vegetation, as well as a common flavor additive in the food industry [12]. Global volatile organic carbon (VOC) emissions studies estimate that 1,150 Tg of biogenic VOC emissions are produced annually, with 10–50 Tg C of this being 2-E-hexanal [13, 14]. For a complete understanding of the effect of

atmospheric processes involving organic peroxy radicals, the effects of water vapor upon the derivatives of E2HEX should not be ignored.

As with isoprene, we expect the first step in the photooxidation of E2HEX under atmospheric conditions to be addition of an OH radical to the double bond [11]. The hydroxylated 2-(E)-hexenal radical then reacts with O_2 to form a family of β-hydroxy peroxy radicals. The general mechanism is described below:

$$OH + C_5H_9CHO \rightarrow C_5H_9(OH)CHO \quad (4)$$

$$C_5H_9(OH)CHO + O_2 \rightarrow C_5H_9(OH)(O_2)CHO \quad (5)$$

Addition of the OH radical can occur on carbons 2 or 3, and the subsequent addition of the peroxy moiety on the opposing carbon results in two chiral centers that may be in either rectus (R) or sinister (S) orientations, resulting in the formation of a family of eight isomers. A second mechanism, although with a much smaller yield, suggests that the OH radical may participate in organic radical formation through hydrogen abstraction [15] as shown below:

$$OH + C_5H_9CHO \rightarrow C_5H_9CO + H_2O. \quad (6)$$

Although this work does not rule out the possibility of this mechanism, the examination of this species will be left to further study. Certainly, comparisons between mechanisms would provide some insight as to the relative abundances of each radical species.

The aim of this work is to demonstrate the existence of E2HEX–H_2O complexes and evaluates the effect of complexation on two representative β-hydroxy peroxy radical isomers derived from E2HEX. The optimized radical geometries and complex binding energies for both isomers are presented.

Methods

The Gaussian 03, Revision D.0110 suite of programs [16] was used to carry out geometry optimizations, vibrational frequency calculations, and high-level configuration interaction molecular energy calculations. The geometry for each radical and radical–water complex was fully optimized at the B3LYP/6-311++G(2d,2p) computational level. Single-point energy calculations were performed at the MP2(full)/6-311++G(2d,2p) level using the optimized geometries found at the B3LYP/6-311++G(2d,2p) level and were used to refine the energy values. Harmonic vibrational frequency calculations performed at the B3LYP/6-311++G(2d,2p) level established each structure as a minimum and allowed for the correction of zero-point energy.

The robust systematic searching method of Clark et al. [11] was used to identify the lowest energy structure for the two hexanal radical isomers (2-hydroxy-3-peroxy hexanal and 2-peroxy-3-hydroxy hexanal radicals). The lowest energy structures of interest in this work were identified by rotating bonds C1—C2, C2—C3, C2—O2(OH), and C3—OH(O2) by 90°, and by rotating bond C3—C4 by 180°. These rotations amounted to 512 unique structures ($[360/90]^4 \times 2$) for each peroxy radical. Structures having nuclei closer than 0.5 Å were ignored. As with Clark et al., the initial optimizations were performed using the HF/6-31G (d,p) method and basis set, followed by further refinement at the B3LYP/6-311++G(d,p) level. The geometry of the 50 lowest energy structures was further refined at the B3LYP/6-311++G(2d,2p) level, and the lowest structure of this group was taken to be the global minimum. Upon identifying the lowest energy geometry of each radical, the optimal complexation arrangement with water was determined using the random constrained sampling method of Clark et al., where 2,000 random radical–water complexes were generated within a 3.5-Å sphere around the aldehyde end of each radical. These complex geometries were then optimized at successively higher methods and basis sets, similar to the process illustrated above, until a lowest energy complex geometry was identified for each radical species. Basis set superposition error was corrected for using the counterpoise procedure.

The optimized geometries and harmonic vibrational frequencies are given in Supporting Information Tables SI–SIV.

Electron density maps with a surface resolution of 0.001 e/au^3 were generated at the MP2(full)/6-311++G(2d,2p)//B3LYP/6-311++G(2d,2p) level for both radical–water complexes. Subtraction of the electron density map computed for the complex from maps for the radical and water alone produced an electron density difference map that reveals the presence of significant electron density shifts that take place upon complexation.

A NBO analysis is instrumental in examining specific intermolecular interactions associated with complex stability. NBO interactions are characterized by donor–acceptor relationships, in which a Lewis-like donor NBO (e.g., lone pair) donates electron density to a non-Lewis-like acceptor NBO (e.g., antibonding orbital). The energy of stabilization, $E^{(2)}$, that arises from electron delocalization can be estimated by second-order perturbation theory that gives a second-order energy, $E^{(2)}$, associated with this interaction, which may be calculated as:

$$E^{(2)} = q_i \left(\frac{(F_{i,j})^2}{\varepsilon_i - \varepsilon_j} \right) \tag{7}$$

where q_i is the donor orbital occupancy, ε_i and ε_j are the diagonal Fock matrix elements describing the energy of the donor and acceptor orbitals, and $F_{i,j}$ is the off-diagonal Fock matrix element describing the energy of interaction between the donor and acceptor orbitals. The second-order perturbation correction for the α- and β-spin orbital components of a given interaction may be summed to provide a reasonable estimate of the interaction energy. $E^{(2)}$ is directly related to the overlap integral $S_{i,j} = \langle \mathrm{NBO_{i,donor}} | \mathrm{NBO_{j,acceptor}} \rangle$ that is estimated from the corresponding preorthogonal NBO, (P)NBO, matrix element. In this work, NBO calculations were conducted at the MP2(full)/6-311++G(2d,2p)//B3LYP/6-311++G(2d,2p) level of theory using the Firefly software package [17] implementation of NBO 5.0 [18].

Thermochemistry data for the radical–water complexes may be extracted from calculated harmonic oscillator frequencies through a standard statistical mechanical treatment [19, 20]. Frequencies for the complexes were calculated at the B3LYP/6-311++G(2d,2p) level and were used to calculate the values of ΔH_{rxn}, ΔS_{rxn}, and ΔG_{rxn} of radical–water complex over the 220–300 K temperature range.

Results and Discussion

β-HYDROXY PEROXY HEXANAL RADICALS

Analysis of the original eight β-hydroxy peroxy hexanal radical conformers, shown in Figure 1, led to the identification of the 2-hydroxy-3-peroxy hexanal (2h3pHEX) and the 2-peroxy-3-hydroxy hexanal (2p3hHEX) radicals. Both 2h3pHEX and 2p3hHEX were chosen to represent the lowest energy structure of each group of four optical isomers. The minimum energy radical–water complex for 2h3pHEX and 2p3hHEX was then identified. The B3LYP/6-311++G(2d,2p)-optimized geometries of each radical and radical–water complex are shown in Figure 2. The binding energies of 2h3pHEX and 2p3hHEX, corrected for zero-point error and basis set superposition error, are shown in Table I.

Complex formation results in structural perturbations to the 2p3hHEX and 2h3pHEX peroxy radical, suggesting that a portion of the stabilization energy arises from charge transfer processes. A useful method for describing how the electron density of each radical delocalizes throughout the entire integrated space defined by the newly formed complex is through electron density difference maps. Maps for the two radical–water complexes discussed here are shown in Figure 3, each with a contour of 0.001 e/au^3, computed at the MP2(full)/6-311++G(2d,2p) level. Blue regions represent areas of electron gain, whereas those of electron loss by red regions. Generally, O—H···O hydrogen bonds are indicated by a region of electron density loss around the proton acceptor atom [21]. Moving along the axis of the hydrogen bond toward the bridging hydrogen atom, a region of electron density gain is then observed followed by another region of electron density loss around the bridging proton. As seen from the electron density shift patterns in Figure 3, two principal H-bonds are present. The first exists between the O atom of H_2O (donor) and the hydroxy function group of the peroxy radical (acceptor). The second is between the aldehyde oxygen atom (donor) and one of the O—H bonds of water. The hydrogen bond lengths and angles of each interaction are listed in Table II. The formation of these new H-bonds breaks the weak interaction that exists between the O—H moiety and the aldehyde in the monomer by rotating the OH proton out of the CCOH plane by $\sim 45^\circ$ to accommodate the H_2O molecule.

The O···H—O interactions of the monomers can be described as a weak hydrogen-bonding interaction, with bond lengths that are $\sim$ 5% (0.1 Å) longer than that found in the H_2O dimer and with bond angles that are strongly acute (i.e., angles that are closer to 90° than 180°). Although the bond lengths for the original hydrogen bonds are close in magnitude, the bond angles differ

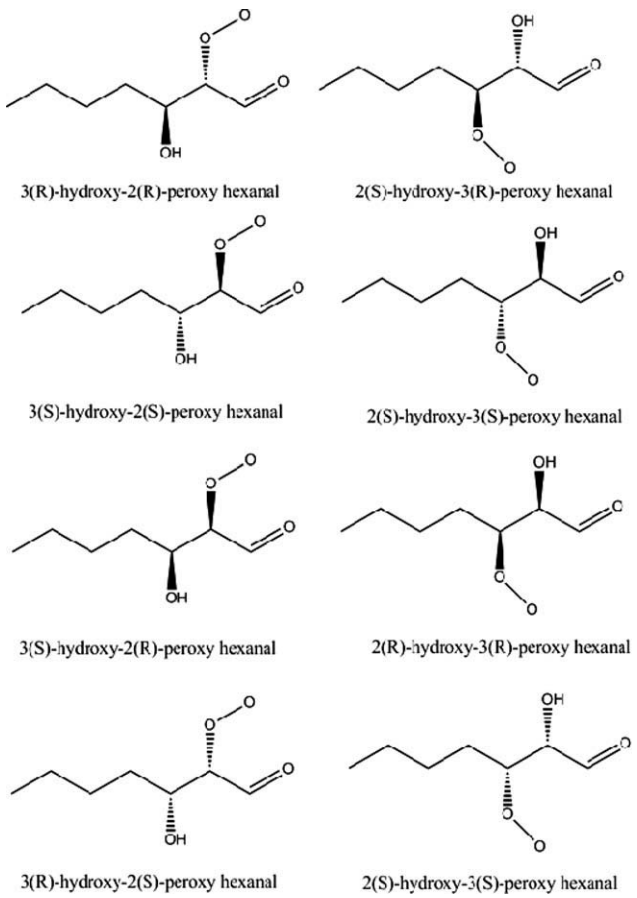

FIGURE 1. Representations of eight possible conformers formed upon serial addition of OH radical and O_2 to 2-E-hexenal. The existence of two chiral center carbons produces a set of four enantiomers with orientations of (*R*, *R*), (*R*, *S*), (*S*, *R*), and (*S*, *S*) for both 2h3pHEX and 2p3hHEX radicals.

markedly. As seen in Figure 1, this is the result of the proximity of the hydroxyl group to the carbonyl oxygen. The placement of OH is in the α-position for 2h3pHEX and is in the β-position for 2p3hHEX. Upon complexation, the nascent hydrogen bonds are replaced by stronger interactions that have shorter bond lengths and bond angles that are closer to the ideal value of 180°. Second-order perturbative estimates, $E^{(2)}$, of the stabilization energy of each hydrogen bond are listed in Table III. In addition, the values of the (P)NBO overlap integrals, which give a measure of the extent of donor NBO and acceptor NBO overlap, are also listed. This data indicate that the hydrogen bond between the water oxygen and the hydroxyl functionality of the radical forms the strongest interaction of the two newly formed H-bonds. The data also indicate that, while present, the second hydrogen bond interaction between the carbonyl oxygen and the water molecule is fairly weak, providing $\sim$ 1 kcal/mol of stabilization energy. The magnitude of this interaction accounts for $\sim$ 70% of the stabilization energy lost upon cleavage of the O—H···O interaction originally present in the monomer. It can be concluded that the stability of the 2p3hHEX–H_2O and 2h3pHEX–H_2O complexes arises principally from the radical–OH···O_w hydrogen bond. The values of the binding energies for these complexes, 3.8 and 3.6 kcal/mol, may appear low, but they are a reflection of the balance between the stabilization lost from the monomer and that gained by the presence of water upon complex formation.

Interestingly, the electron density difference maps, Figure 3, indicate a lack of significant intermolecular interactions between the water and the peroxy moiety in either of the 2h3pHEX or 2p3hHEX radicals. Although small electron density shifts are evident in the O—O—C region of the radical, there is no significant interaction

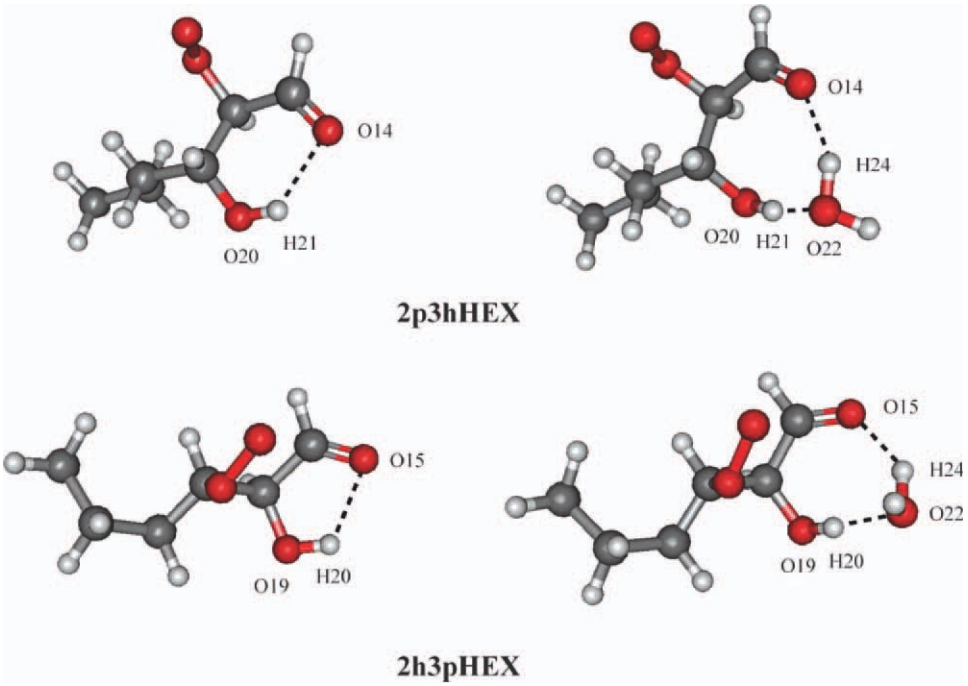

FIGURE 2. Optimized geometries of the 2p3hHEX and 2h3pHEX and the associated water complexes as determined at the B3LYP/6-311++G (2d,2p) level. [Color figure can be viewed in the online issue, which is available at wileyonlinelibrary.com.]

observed between these shifts and those associated with the two primary hydrogen bonds. The NBO analysis indicates that the peroxy moiety plays no role in the overall stability of the radical–water complexes, which is in stark contrast with interactions observed in HIPs and smaller organic peroxy radical complexes where the peroxy moiety plays a central role complex stabilization. It is of note that smaller peroxy radicals containing an aldehyde group, such as the acetyl and acetonyl peroxy radicals, also indicate a lack of interaction between the carbonyl carbon and the peroxy functionalities [10].

THERMOCHEMISTRY

The relevance of the 2p3hHEX and 2h3pHEX complex systems at atmospherically relevant temperatures is analyzed through thermochemical calculations. The resulting data are presented in Table IV.

As expected, complex formation requires a loss of entropy as the radical and the H_2O molecule form a stable bound complex. The loss of entropy is minor, amounting to $\sim$ 0.03 kcal/mol/K. It is also apparent from the data in Table IV that the formation of both complexes is enthalpically favored over the temperature range of interest. The magnitude of

TABLE I

Zero point energy (ZPE)-corrected binding energies of hydroxy peroxy hexanal-water complexes, adjusted for basis set superposition error (BSSE).

	ΔE(kcal/mol)				
Complex	ZPVE	BSSE	B3LYP[a]	MP2(full)[a]	MP2(full)corr
2p3hHEX + H_2O	120.6				0.0
2p3hHEX–H_2O	122.6	2.0	−6.0	−7.8	−3.8
2h3pHEX + H_2O	120.6				0.0
2h3pHEX–H_2O	122.6	2.2	−6.1	−7.8	−3.6

[a] Denotes 6–311++G(2d,2p).

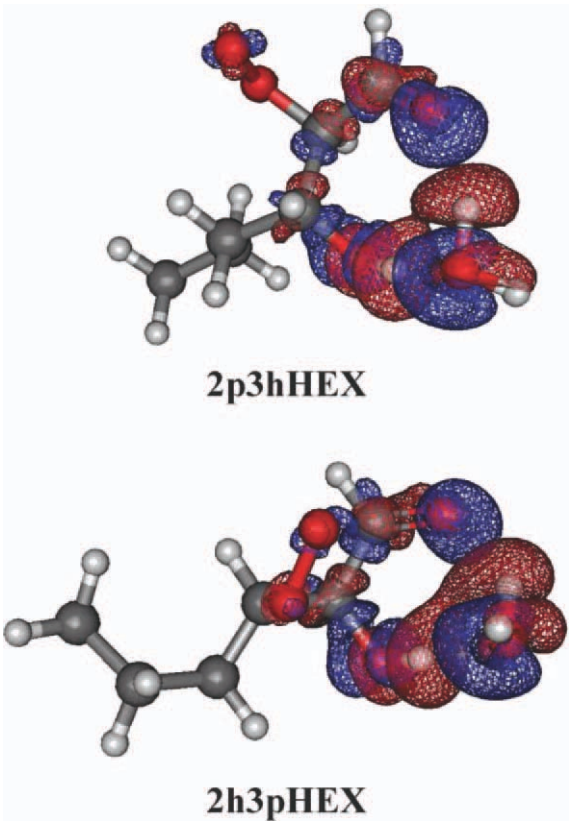

FIGURE 3. Electron density difference maps for 2p3hHEX and 2h3pHEX, with a contour of 0.001 e/au^3 calculated at the UMP2(full)/6-311G++(2d,2p) level. Blue shaded regions represent areas of electron density gain, and red shaded regions represent areas of electron loss, relative to the isolated subunits. [Color figure can be viewed in the online issue, which is available at wileyonlinelibrary.com.]

the Gibb's free energy at each temperature point indicates that the formation of 2h3pHEX–H_2O and 2p3hHEX–H_2O can readily occur.

TABLE II

Hydrogen bond lengths and angles for 2p3hHEX and 2h3pHEX and the associated water complexes.

Complex	Interaction	r(H···O) (Å)	θ(OHO) (○)
2p3hHEX	O20—H21···O14	2.082	132.4
2p3hHEX–H_2O	O20—H21···O14	2.844	98.3
	O20—H21···O22	1.844	168.8
	O22—H24···O14	1.955	151.6
2h3pHEX	O19—H20···O15	2.052	118.1
2h3pHEX–H_2O	O19—H20···O15	2.587	93.6
	O19—H20···O22	1.831	170.3
	O22—H24···O15	2.020	143.2

TABLE III

The $E^{(2)}$ and S nσ^* descriptors of the hydrogen bonds in 2p3hHEX and 2h3pHEX radicals and the associated water complexes.

Complex	Interaction	$E^{(2)}$ (kcal/mol)	S nσ^*
2p3hHEX	O20—H21···O14	1.43	0.1388
2p3hHEX–H_2O	O20—H21···O14	-	-
	O20—H21···O22	6.95	0.2732
	O22—H24···O14	1.01	0.1141
2h3pHEX	O19—H20···O15	1.48	0.1482
2h3pHEX–H_2O	O19—H20···O15	-	-
	O19—H20···O22	7.78	0.2844
	O22—H24···O15	1.07	0.1186

Useful information regarding the atmospheric abundance of these peroxy radical–water complexes at different values for the relative humidity can be obtained in terms of a ratio between complexed and uncomplexed peroxy radicals by multiplying the equilibrium constant by the relevant [H_2O] concentration, as shown in Eq. (8)

$$K_{eq}[H_2O] = \frac{[RO_2 \cdot H_2O]}{[RO_2]} \tag{8}$$

TABLE IV

Thermodynamic properties, ΔH_{rxn}, ΔS_{rx}, and ΔG_{rxn}, calculated for the formation of the 2p3hHEX–H_2O and 2h3pHEX–H_2O complexes at the B3LYP/6–311++G(2d,2p) level.

TEMP (K)	ΔH_{rxn} (kcal mol)	ΔS_{rxn} (cal mol K)	ΔG_{rxn} (kcal mol)
2h3pHEX–H_2O			
220	−4.51	−0.03	−4.51
230	−4.50	−0.03	−4.50
240	−4.49	−0.03	−4.48
250	−4.47	−0.03	−4.47
260	−4.46	−0.03	−4.45
270	−4.44	−0.03	−4.43
280	−4.42	−0.03	−4.41
290	−4.40	−0.03	−4.40
300	−4.38	−0.03	−4.37
2p3hHEX–H_2O			
220	−4.51	−0.03	−4.51
230	−4.50	−0.03	−4.50
240	−4.49	−0.03	−4.48
250	−4.47	−0.03	−4.47
260	−4.46	−0.03	−4.45
270	−4.44	−0.03	−4.43
280	−4.42	−0.03	−4.41
290	−4.40	−0.03	−4.40
300	−4.38	−0.03	−4.37

The equilibrium constant for the formation of each complex and the $K_{eq}[H_2O]$ ratio are tabulated in Table V, and the results of Eq. (8) are displayed in Figure 4, which shows a plot of this ratio as a function of temperature at 100% humidity.

As expected, the relative abundance of the complex increases relative to the uncomplexed peroxy radical as the abundance of atmospheric moisture increases with temperature. The $K_{eq}*[H_2O]$ ratio values are indicative of other peroxy–water systems, such as the methyl peroxy, ethyl peroxy, and the acetyl peroxy radicals [10]. One noticeable difference between the 2h3pHEX–H_2O and 2p3hHEX–H_2O complexes and those mentioned in Ref. [8] is the larger corrected binding energies, $\sim$ 1 kcal/mol, of the E2HEX-derived peroxy radicals. The larger binding energies can be attributed to the presence of the hydroxyl group and not the carbonyl. In addition, the extra carbon bulk of the E2HEX peroxy radicals distant from the hydrogen bonding region seems to play no role in the stabilization of RO_2 radicals. When the logarithm of the $K_{eq}*[H_2O]$ ratio is plotted against temperature an almost linear relationship is observed. This is consistent with the water vapor concentration increasing exponentially with warming temperatures. Many atmospheric modeling studies have ignored the water influence on RO_2 abundances and RO_2 chemistry. If the presence of water can be shown to perturb either of the reaction rate constant of any reactions involving 2h3pHEX or 2p3hHEX or any of the resulting product branching ratios, the formation of these complexes will be important in our understanding of atmospheric oxidative pathways. Although experimental studies will be necessary to corroborate these theoretical findings, it is anticipated that these complexes will play a primary role in the atmospheric stability of hydroxy-peroxy hexanal radicals.

TABLE V

Equilibrium constants and the $K_{eq}[H_2O]$ ratio calculated for the formation of the 2p3hHEX$-H_2O$ and 2h3pHEX$-H_2O$ complexes at the B3LYP/6–311++G(2d,2p) level.

TEMP (K)	K_{eq}	$K_{eq}*[H_2O]$(RH=100%)
2h3pHEX$-H_2O$		
220	1.46×10^{-20}	1.68×10^{-05}
230	8.11×10^{-21}	2.56×10^{-05}
240	4.76×10^{-21}	4.00×10^{-05}
250	2.92×10^{-21}	6.55×10^{-05}
260	1.86×10^{-21}	1.03×10^{-04}
270	1.23×10^{-21}	1.57×10^{-04}
280	8.42×10^{-22}	2.19×10^{-04}
290	5.92×10^{-22}	2.87×10^{-04}
300	4.27×10^{-22}	3.68×10^{-04}
2p3hHEX–H_2O		
220	3.87×10^{-20}	4.46×10^{-05}
230	2.18×10^{-20}	6.87×10^{-05}
240	1.29×10^{-20}	1.08×10^{-04}
250	7.97×10^{-21}	1.79×10^{-04}
260	5.13×10^{-21}	2.84×10^{-04}
270	3.42×10^{-21}	4.37×10^{-04}
280	2.36×10^{-21}	6.12×10^{-04}
290	1.67×10^{-21}	8.09×10^{-04}
300	1.21×10^{-21}	1.04×10^{-03}

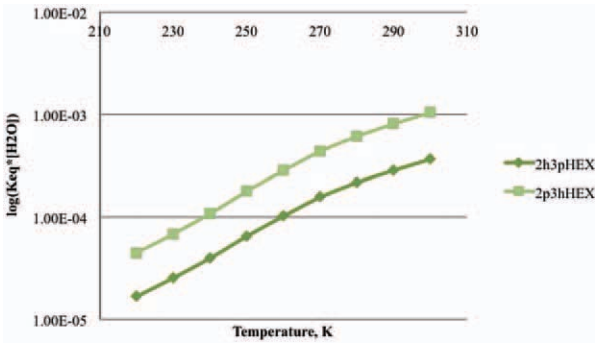

FIGURE 4. The ratio of [radical–H_2O]/[radical] as calculated for 2h3pHEX and 2p3hHEX at the B3LYP/6-311++G(2d,2p) level. The water concentration used was that exists at a relative humidity of 100% at the included temperatures. [Color figure can be viewed in the online issue, which is available at wileyonlinelibrary.com.]

Conclusion

Owing to the significant contribution of E-2-hexenal to the total biogenic VOC emissions in the atmosphere, the contribution of radicals derived from this species is an important step toward understanding tropospheric chemistry. This work demonstrates an expected binding energy between hydroxy peroxy hexanal radicals and water that is comparable with previous organic radical studies. Primary intermolecular interactions within the complex are attributed to hydrogen bonds between water and the hydroxy and aldehyde moieties of the radical, with the peroxy group playing only a slight role in complex stability. The additional carbon bulk of the 2h3pHEX and 2p3hHEX radicals seems to play no part, for

good or bad, in the stabilization of the radicals, indicating that binding motifs identified for smaller RO_2 radicals are relevant to larger molecular weight peroxy radicals. Thermochemical calculations demonstrate that the formation of these complexes is favorable, with the Gibb's free energy of formation in excess of 4 kcal/mol, and that they are likely to exist at all of the atmospherically relevant temperatures studied. The ratio of complexed radical to noncomplexed radical is similar to less functionalized smaller RO_2 radicals that have been studied previously. Owing to the possible importance of these complexes in the atmosphere, this study highlights the need for experimental validation of these complexes under atmospheric conditions.

ACKNOWLEDGMENT

The authors thank the Ira and Marylou Fulton Supercomputing Laboratory at BYU for supercomputer time. Undergraduate support was provided by the BYU-Idaho Academic Office, the BYU-Idaho College of Physical Sciences and Engineering Undergraduate Research, and the Talmage Fellowship program sponsored by the Department of Chemistry and Biochemistry at Brigham Young University. They also thank the reviewers for their helpful comments.

References

1. Suma, K.; Sumiyoshi, Y.; Endo, Y. Science 2006, 311, 1278.
2. Aloisio, S.; Francisco, J. S. J Phys Chem A 1998, 102, 1899.
3. Lightfoot, P. D.; Veyret, B.; Lesclaux, R. J Phys Chem 1990, 94, 708.
4. Tang, Y.; Tyndall, G. S.; Orlando, J. J. J Phys Chem A 2009, 114, 369.
5. Hamilton, E. J.,Jr.; Lii, R. R. Int J Chem Kinet 1977, 9, 875.
6. Hamilton, E. J.,Jr. J Chem Phys 1975, 8, 3682.
7. Butkovskaya, N.; Rayez, M.-T. r. s.; Rayez, J.-C.; Kukui, A.; Le Bras, G. J Phys Chem A 2009, 113, 11327.
8. Gonzalez, J.; Torrent-Sucarrat, M.; Anglada, J. M. Phys Chem Chem Phys 2010, 12, 2116.
9. Long, B.; Tan, X.-f.; Ren, D.-s.; Zhang, W.-j. Chem Phys Lett 2010, 492, 214.
10. Clark, J. M.; Hansen, J. C.; English, A. M.; Francisco, J. S. J Phys Chem A 2008, 112, 1587.
11. Clark, J.; Call, S. T.; Austin, D.; Hansen, J. C. J Phys Chem A 2010, 114, 6534.
12. Lanciotti, R.; Belletti, N.; Patrignani, F.; Gianotti, A.; Gardini, F.; Guerzoni, M. E. J Agric Food Chem 2003, 51, 2958.
13. Guenther, A. Reactive Hydrocarbons in the Atmosphere; Academic Press: San Diego, 1999.
14. Wiedinmyer, C.; Guenther, A.; Harley, P.; Hewitt, C. N.; Geron, C.; Artaxo, P.; Steinbrecher, R.; Rasmussen, R. Emissions of Atmospheric Trace Compounds; Kluwer Academic Publishers: Dordrecht, 2004.
15. Albaladejo, J.; Ballesteros, B.; Jimenez, E.; Martin, P.; Martinez, E. Atmos Environ 2002, 36, 3231.
16. Frisch, M. J.; Trucks, G. W.; Schlegel, H. B.; Scuseria, G. E.; Robb, M. A.; Cheeseman, J. R.; Montgomery, J. A.,Jr.; Vreven, T.; Kudin, K. N.; Burant, J. C.; Millam, J. M.; Iyengar, S. S.; Tomasi, J.; Barone, V.; Mennucci, B.; Cossi, M.; Scalmani, G.; Rega, N.; Petersson, G. A.; Nakatsuji, H.; Hada, M.; Ehara, M.; Toyota, K.; Fukuda, R.; Hasegawa, J.; Ishida, M.; Nakajima, T.; Honda, Y.; Kitao, O.; Nakai, H.; Klene, M.; Li, X.; Knox, J. E.; Hratchian, H. P.; Cross, J. B.; Bakken, V.; Adamo, C.; Jaramillo, J.; Gomperts, R.; Stratmann, R. E.; Yazyev, O.; Austin, A. J.; Cammi, R.; Pomelli, C.; Ochterski, J. W.; Ayala, P. Y.; Morokuma, K.; Voth, G. A.; Salvador, P.; Dannenberg, J. J.; Zakrzewski, V. G.; Dapprich, S.; Daniels, A. D.; Strain, M. C.; Farkas, O.; Malick, D. K.; Rabuck, A. D.; Raghavachari, K.; Foresman, J. B.; Ortiz, J. V.; Cui, Q.; Baboul, A. G.; Clifford, S.; Cioslowski, J.; Stefanov, B. B.; Liu, G.; Liashenko, A.; Piskorz, P.; Komaromi, I.; Martin, R. L.; Fox, D. J.; Keith, T.; Al-Laham, M. A.; Peng, C. Y.; Nanayakkara, A.; Challacombe, M.; Gill, P. M. W.; Johnson, B.; Chen, W.; Wong, M. W.; Gonzalez, C.; Pople, J. A. Gaussian 2003, Revision D.0110, Gaussian, Inc.: Wallingford, CT, 2004.
17. Granovsky, A. A. 2010. GAMESS/Firefly Version 7.1.G, http://classic.chem.msu.su/gran/firefly/index.html.
18. Glending, E.; Lanids, C. R.; Weinhold, F. Theoretical Chemistry Institute and Department of Chemistry: Madison, WI, 2010.
19. Ochterski, J. 2000. http://www.gaussain.com/g_whitepap/thermo.htm.
20. McQuarrie, G. Z.; Simon, J. D. Physical Chemistry: A Molecular Approach; University Science Books, Mill Valley, CA, 1997.
21. Yanling, G.; Tapas, K.; Scheiner, S. J. J Am Chem Soc 1999, 121, 9411.